Journal of Asian Ceramic Societies

ISSN: (Print) 2187-0764 (Online) Journal homepage: https://www.tandfonline.com/loi/tace20

Starch consolidation of SiC ceramics: processing and low-temperature sintering in an air atmosphere

Ayse Kalemtas, Gülsüm Topates, M. Türkay Aytekin Aydin & Nigar Özey

To cite this article: Ayse Kalemtas, Gülsüm Topates, M. Türkay Aytekin Aydin & Nigar Özey (2020) Starch consolidation of SiC ceramics: processing and low-temperature sintering in an air atmosphere, Journal of Asian Ceramic Societies, 8:1, 106-115, DOI: 10.1080/21870764.2019.1710017

To link to this article: https://doi.org/10.1080/21870764.2019.1710017

JOURNAL OF ASIAN CERAMIC SOCIETIES
2020, VOL. 8, NO. 1, 106–115
https://doi.org/10.1080/21870764.2019.1710017

FULL LENGTH ARTICLE

OPEN ACCESS

Starch consolidation of SiC ceramics: processing and low-temperature sintering in an air atmosphere

Ayse Kalemtas[a], Gülsüm Topates[b], M. Türkay Aytekin Aydin[c] and Nigar Özey[d]

[a]Department of Metallurgical and Materials Engineering, Bursa Technical University, Bursa, Turkey; [b]Department of Metallurgical and Materials Engineering, Ankara Yıldırım Beyazit University, Ankara, Turkey; [c]Department of Physics, Science Faculty, Eskisehir Technical University, Eskisehir, Turkey; [d]Bosch, Bursa, Turkey

ABSTRACT

Highly porous SiC ceramics containing borax decahydrate were produced by a starch consolidation method in which corn starch was used as a shaping and pore-forming additive. Four different compositions were prepared with different SiC:borax decahydrate ratios and corn starch content. Mixtures with a solid ratio of 55 wt.% were cast in non-porous molds and heated at 80°C for shaping. The starch consolidation technique enabled the shaping of SiC ceramics with different forms and sizes. Simultaneous thermogravimetry and differential thermal analysis of the SiC-borax decahydrate mixture showed that melting took place at below 600°C, as a result of which sintering was carried out at the relatively low temperature, of 600°C in the air using borax decahydrate as a sintering additive. Phase analysis showed that oxidation of SiC did not take place, since no cristobalite phase was detected. Density measurement and mercury porosimetry studies showed that highly porous (70–89% porosity) SiC ceramics with pore size values ranging from 14 to 18 µm were produced. SEM microstructures of each composition revealed that a strong neck had been formed between the SiC particles in spite of the low sintering temperature.

ARTICLE HISTORY
Received 7 September 2019
Accepted 18 December 2019

KEYWORDS
Starch consolidation; Porous SiC; TG–DTA; Sintering under atmospheric conditions; Low–temperature sintering

1. Introduction

Porous ceramics, especially highly porous SiC ceramics, have received significant attention recently because of their attractive properties such as low density; high surface area; good chemical stability; and high-temperature stability; low thermal expansion coefficient; good wear oxidation corrosion, and thermal shock resistance; controlled permeability; excellent high-temperature strength and catalytic activity; high thermal conductivity; and superior mechanical properties such as high specific strength and hardness [1–6]. Porous SiC ceramics have been considered as potential candidate materials for various technological applications, including hot-gas and molten metal filters, electrodes, heat exchangers, thermal insulating materials, diesel particulate filters, membrane and catalyst supports, vacuum chucks, gas burner media, sensors, refractory materials, preforms for composite fabrication, and lightweight structural materials [4–15]. The sintering steps in porous SiC ceramic production have generally been carried out under controlled atmospheres such as nitrogen or argon and at high temperatures due to the non-oxide and strongly covalent nature of the Si–C bonds. Due to these features, practical applications and market opportunities of porous SiC–based ceramics are limited. Thus, fabrication of highly porous SiC-based ceramics at low sintering temperatures, without the need of expensive additives, instrumentation and controlled atmospheres has recently become a challenging issue for researchers.

Many researchers have already expended extensive efforts to produce porous SiC ceramics at low sintering temperatures and in an air atmosphere. She et al. [16–18] have developed a novel approach, an oxidation-bonding technique, for the manufacture of porous SiC ceramics at relatively low sintering temperatures, 1100–1400°C for 1 h, and in an air atmosphere. In these studies, SiC particles were bonded by oxidation-derived silica glass, and it was observed that the oxidation–bonded porous SiC ceramics produced had excellent oxidation resistance, large surface areas, high flexural strength, good thermal shock resistance and Weibull modulus [16–18]. Zhu et al. produced SiC-reticulated porous ceramics by utilizing oxidation-derived silica to bond the ceramic particles [19]. Due to the aforementioned limitations of porous SiC fabrication, some researchers utilized another approach, in situ reaction bonding, to produce porous SiC ceramics at low sintering temperatures in an air atmosphere. In this approach, bonding of the SiC particles was achieved by the addition of secondary phases into the system, which forms mullite, cordierite other such phases at elevated temperatures [20–28]. To produce mullite-bonded porous SiC ceramics, for instance, Al_2O_3 might be added to the SiC starting powder. During

CONTACT Ayse Kalemtas ayse.kalemtas@btu.edu.tr Department of Metallurgical and Materials Engineering, Bursa Technical University, Bursa, Turkey

the sintering process in an air atmosphere, the surface of the SiC particles is oxidized to SiO_2 and reacts with Al_2O_3 to form a mullite bonding phase [20]. Lim et al. produced highly porous (47–64%) SiC ceramics using borax decahydrate ($Na_2B_4O_7 \cdot 10H_2O$) as a bonding phase in a simple pressing and heat–treatment process. Porous SiC ceramics were sintered at low temperatures (600–800°C) in an air atmosphere using borax decahydrate as a sintering aid and starch as a fugitive additive. The SiC to borax decahydrate weight ratio was kept constant as 4:1, and the effects of the applied sintering temperature and starch amount (40–46 wt%) on the porosity and strength of the porous SiC ceramics were investigated [29].

A great deal of effort has been devoted to the fabrication of highly porous SiC-based ceramics using various techniques, such as a polymeric sponge technique [19,30], use of fugitive additives [31], partial hot-pressing [32,33], gel-casting [34–36], sintering of hollow spheres as sacrificial templates [37], sol–gel and carbothermal reduction [38,39], pyrolysis and infiltration of natural wood precursors [40,41], freeze-casting and solid-state sintering [42–44], a liquid infiltration technique [45–47] and direct foaming of ceramic suspensions or preceramic polymers [48–52]. Depending on the processing technique selected, porosity content achieved, pore size distribution, and degree of pore interconnectivity factors which have direct effects on the properties of the porous ceramic are varied. Among the approaches taken in the recent focus on a novel processing of porous ceramics, the starch consolidation technique has attracted significant attention due to its near-net shaping capability without requiring specialized equipment, its ease of processing, and its cost-effectiveness [53–69]. Also, components from simple to complex shapes can be produced by this technique. Furthermore, the starch consolidation technique ensures a highly systematic approach to designing the microstructures of the ceramics by controlling the content of the slurry used in the solid loading, the amount and source of the starch used, degree of sintering conducted during the heat treatment step. The size of the starch depends on the type of changes it undergoes between 2 and 170 μm [53]. Thus, it is possible to achieve a relatively wide range of pore sizes via starch consolidation technique. It is reported in the literature that macroporous SiC ceramics with smaller pores generally exhibit higher flexural strength when compared with SiC ceramics with larger pores and an equivalent porosity content [70,71].

The objective of the present current study was to produce highly porous cristobalite-free SiC-based ceramics via a relatively novel shaping technique for porous SiC fabrication, the starch consolidation technique. It was, moreover aimed at achieving sintering at very low temperatures (≤600°C for 1 h) and in an air atmosphere to expand the range of applications of these porous ceramics.

2. Experimental procedure

The starting materials consisted of SiC (357,391, Aldrich, d_{50} = 24.8 μm), borax decahydrate ($Na_2B_4O_7.10H_2O$, Tekkim, d_{50} = 32.9 μm) corn starch (Piyale) and kaolinite (as a binder in the amount of 2.5 wt.%, CC31, Esan – Eczacıbaşı). SEM images of SiC and the corn starch are shown in Figure 1(a,b). SiC contains sharp-angled particles, and starch particles have irregular shapes with a narrow size distribution varying from 10 to 20 μm.

Four compositions with different SiC/borax decahydrate ratios and starch amounts were prepared (as given in Table 1). The solid loading content was fixed at 55 wt.%. Owing to the higher dissolution of borax decahydrate in water, planetary ball-milling was limited for 15 min at 400 rpm.

The starch, borax decahydrate and mixture of SiC and borax decahydrate were analyzed by TG-DTA analysis (Netzsch STA 449 F3) up to 700°C with a heating rate of 10°C/min to identify possible weight changes and reactions occurring during the sintering process.

The slurries were cast in non-porous molds, and aged in a drying oven at 80°C for 1 h for water absorption and further swelling of the starch. After the shaping process, the samples were removed from the molds and then both heat–treated and sintered at 600°C for 1 h in air.

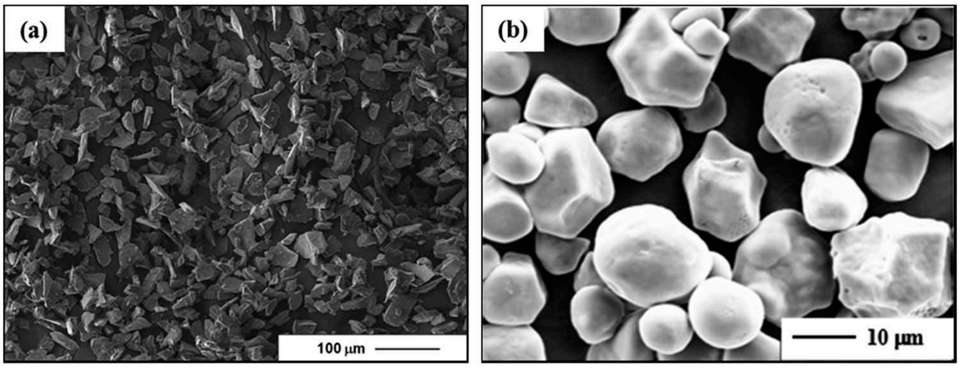

Figure 1. SEM images of (a) SiC and (b) corn starch particles.

Table 1. Composition denominations and amount of starting materials.

Denomination	SiC (wt.%)	Borax decahydrate (wt.%)	Starch (wt.%)
SC70S30–3*	56.77	18.90	24.33
SC70S30–5	61.40	12.28	26.32
SC50S50–3	42.88	14.24	42.88
SC50S50–5	45.46	9.09	45.45

SC: SiC, S: starch and *: this number gives the ratio of SiC to borax decahydrate.

The heating rate applied was 1°C/min and the cooling rate was 3°C/min. The weight volume ratios of the samples were measured for density calculation.

Samples were identified by X-ray diffraction (XRD, D8 Advance, Bruker Instrument Co., Ltd., Germany) to observe the phase composition using Cu–Kα radiation for 2θ values from 20° to 80°. The sintered samples were ground down to 63 µm before XRD analysis. Their pore size and distribution were characterized using a mercury intrusion porosimeter (Quantachrome Pore Master-60). The microstructures of the porous SiC ceramics were characterized by SEM (FESEM, ZEISS Ultraplus, Germany). Elemental investigations of the liquid phase were performed using SEM with energy dispersion X-ray spectrometry (SEM-EDX, Hitachi SU5000, Japan).

3. Results and discussions

The TG-DTA analysis of the corn starch in Figure 2 shows that mass loss occurred at three different temperatures. Dehydration occurred at 115°C accompanying a mass loss of around 11.20%. There are two types of polysaccharides in the starch: amylose and amylopectin. The second mass loss formed at between 275°C and 325°C as a 65.29% mass loss after burning out of the amylopectin groups. The amylose group was released between 325°C and 525°C and the mass loss was 22.66%. TG-DTA shows that starch was completely removed from the samples before reaching the sintering temperatures.

Gradual removal of water from the borax decahydrate was observed in the TG-DTA curves given in Figure 3. Following two endothermic reactions occurring at 114° and 156°C, ~46% weight loss was attained through water evaporation. The theoretical weight loss was 47.2% for borax, with the presence of impurities as the reason for the slight decrease in the weight loss value. The exothermic reaction at 606°C showed crystallization of the anhydrous sodium borate.

A starch consolidation technique was employed to shape the SiC ceramics in various forms from thicker cross-sections (Figure 4(a)) to complex shapes (Figure 4(b–d)). During the soaking of the samples at 80°C, the starch granules were swollen due to absorption of the water. Since the volume of water was reduced, the distance between SiC particles decreased bringing them into contact, and eventually a solid network was formed. The swollen starch granules acted as a binder, moreover, increasing the green strength and easing the removal of the green ceramics from the mold [72].

TG-DTA analysis (Figure 5) of the SiC-borax decahydrate mixture with a ratio of 3:1 had two endothermic peaks at 92°C and 140°C which occurred during the dehydration of the crystal water from the borax decahydrate. No crystallization of anhydrous sodium borate was observed as it was mixed with SiC. The SiC suppressed the crystallization of this phase. At 656°C, melting took place through an endothermic reaction. Since the onset temperature of the melting reaction was below 600°C, formation of the liquid phase took place at the sintering temperature of the samples via a reaction between the oxide layer present on the surface of the SiC grains and the anhydrous sodium borate.

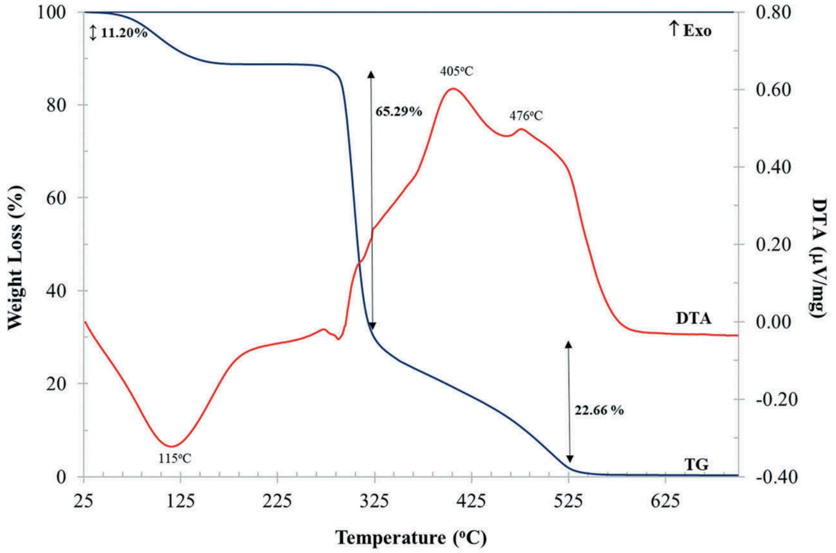

Figure 2. TG-DTA analysis of corn starch.

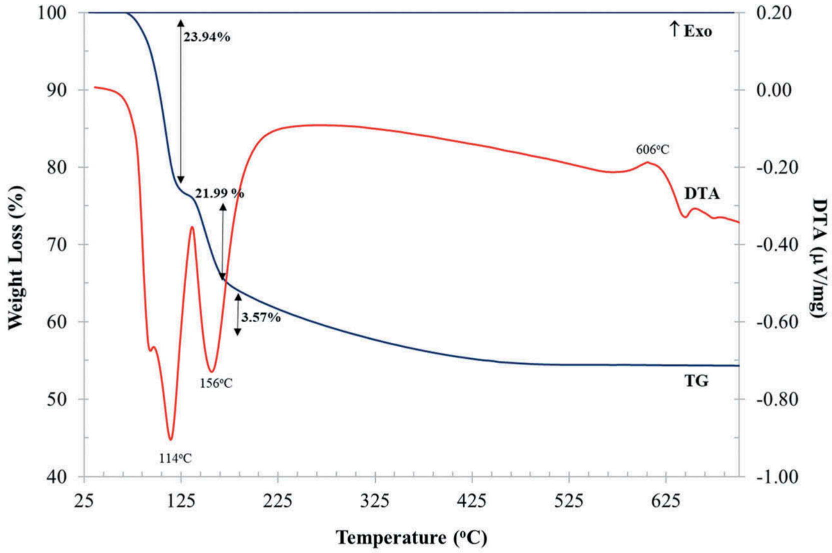

Figure 3. TG-DTA analysis of borax decahydrate.

The XRD patterns of samples sintered at 600°C can be seen in Figure 6. The only crystal phase identified was SiC. Despite the larger amount of borax decahydrate, no peak of this phase was observed. This confirmed that SiC inhibited the crystallization of borax decahydrate as observed in TG-DTA analyses.

According to mercury intrusion porosimetry analysis (Figure 7), all the samples had a monomodal pore size distribution in which the pore size changed from 7 to 20 µm. No significant contribution of the composition and sintering temperatures on the pore characteristics was observed. The highest mean pore size obtained was 18 µm for SC70S30–3 sintered at 600°C.

The microstructures of the samples had different compositions from the fracture surfaces as given in Figure 8(a–h). Two types of pores were observed: interparticle pores formed between the SiC grains (indicated by yellow circles) and a second type of pores that appeared after the burn-out of starch particles (indicated by red circles). Also, the addition of starch-developed channel-like continuous pore structures as seen in Figure 8(c). As the ratio of SiC to borax decahydrate increased, more porous structures were developed. A more porous region was observed in Figure 8(g) than in Figure 8(e). A larger amount of borax decahydrate increased the amount of liquid phase formed and promoted densification of the samples. Furthermore, a strong neck formation (indicated by arrows in Figure 8(d)) took place in all the compositions. Formation of a liquid phase through the melting of borax decahydrate and a reaction of this phase with the SiO_2 surface oxide layer of SiC enhanced the bonding of the SiC grains and a consolidated structure was obtained even at very low sintering temperatures. The effect of the starch is quite apparent in Figure 8(c,e). A less porous region formed after the burn-out of starch was observed when the amount of starch decreased from 50% to 30%. A new type of porosity was formed around those grains whose size was finer (less than 1 µm) compared to the other porosities. As seen in Figure 8(f) nearly spherical pores developed during the evaporation of the finer starch particles and crystal water of borax decahydrate from the liquid phase, and this finer pores appeared. The ratio of SiC to borax decahydrate is critical to obtain well-bonded SiC grains, as seen in Figure. 8(b,f). At higher SiC borax decahydrate ratios (for SC70S30–3 and SC50S50–3) coalescence of the SiC grains (indicated by arrows) occurred through the liquid borax decahydrate phase.

The composition of the liquid phase was investigated by an SEM-EDX mapping study of all the samples. A representative SEM image and an elemental map analysis of an SC70S30–3 sample are presented in Figure. 9(a,b), respectively. The elemental maps confirmed the presence of B in the liquid phase. A homogenous distribution of borax decahydrate was observed due to the uniform liquid presence in the microstructure. Besides B, Na and O (from borax decahydrate), Si, C and Al (from kaolinite) were detected. Table 2 shows the elemental composition of all samples from the SEM-EDX mapping study. In all the samples, B was detected with the amount varied from 5.0 to 6.0 in wt.%.

4. Conclusions

- In the current study starch consolidation, a direct consolidation technique was successfully applied

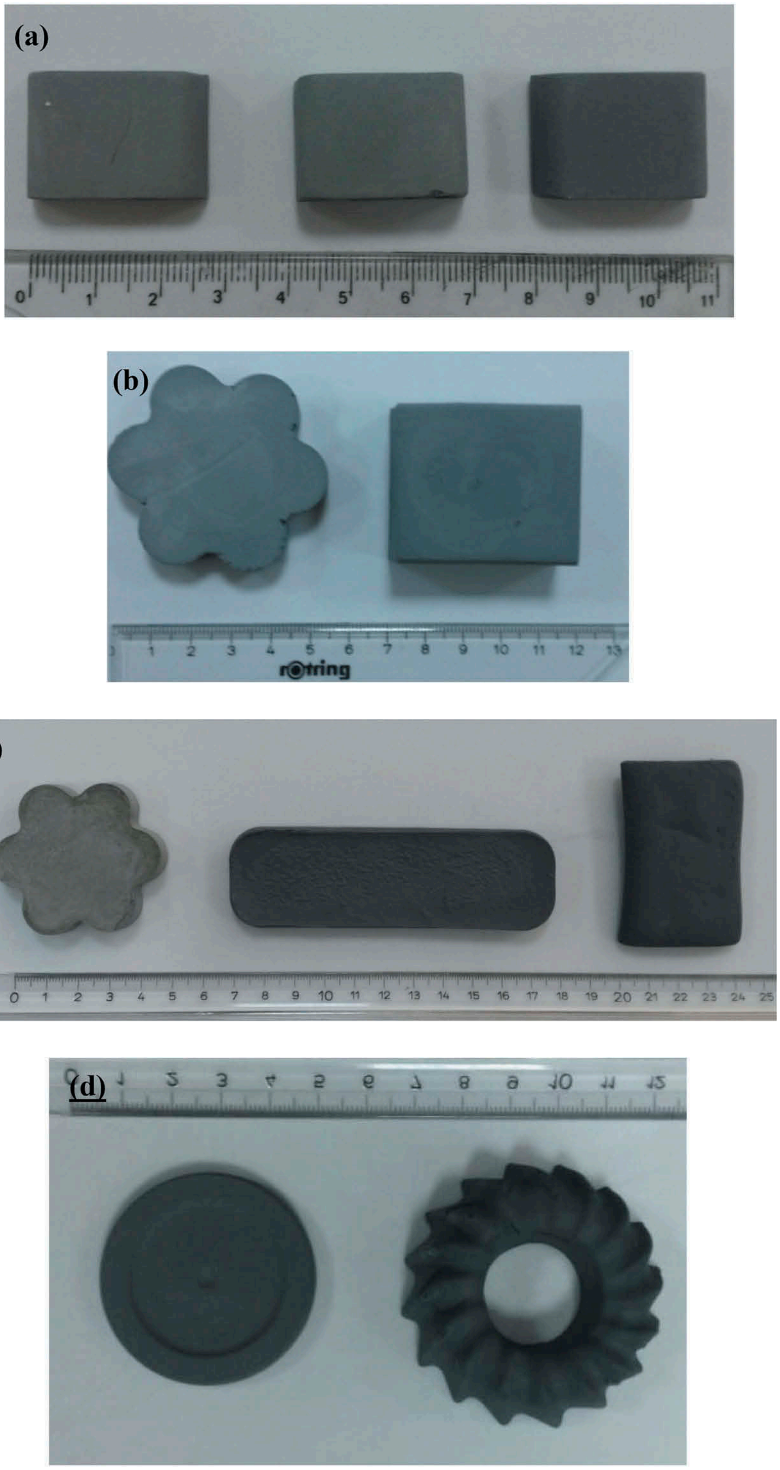

Figure 4. Samples with various forms shaped by starch consolidation (a, b) and sintered (c, d) at 600°C.

to fabricate highly porous SiC ceramics. The starch acted as a pore-forming and body-forming agent in the system.

- There are two types of pores in the system, one of them derived from the burn-out of the starch grains and the other due to the stacking of SiC powder particles.
- Sintering studies were carried out in an air atmosphere and at relatively low sintering temperatures. XRD analysis confirmed that cristobalite-free porous SiC ceramics were successfully produced at low sintering temperatures and in an air atmosphere.
- Scanning electron microscopy investigations revealed that the porous ceramic structure was highly homogenous and that strong neck formations were achieved between SiC grains due to a large amount of the liquid phase in the system. Use of a borax decahydrate ($Na_2B_4O_7.10H_2O$) sintering additive and its reaction with the surface silica content of the SiC ceramic powders resulted in the

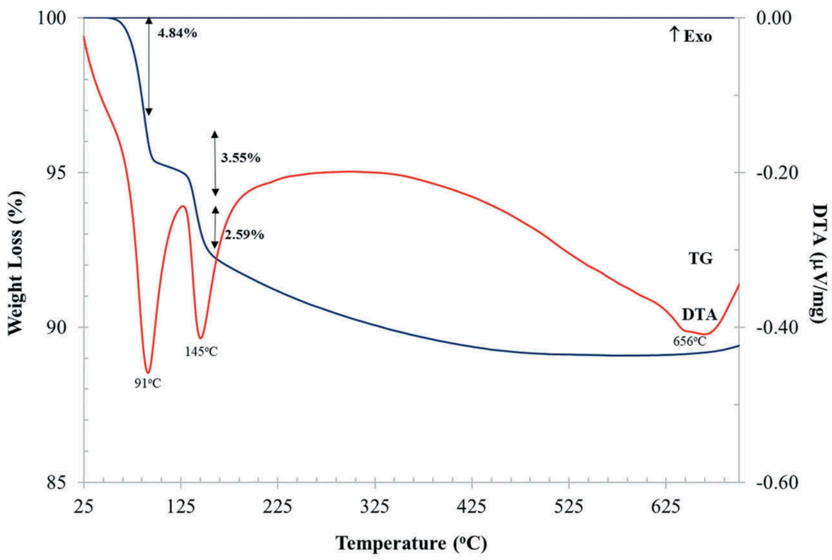

Figure 5. TG-DTA analysis of the mixture SiC-borax decahydrate with a ratio of 3:1.

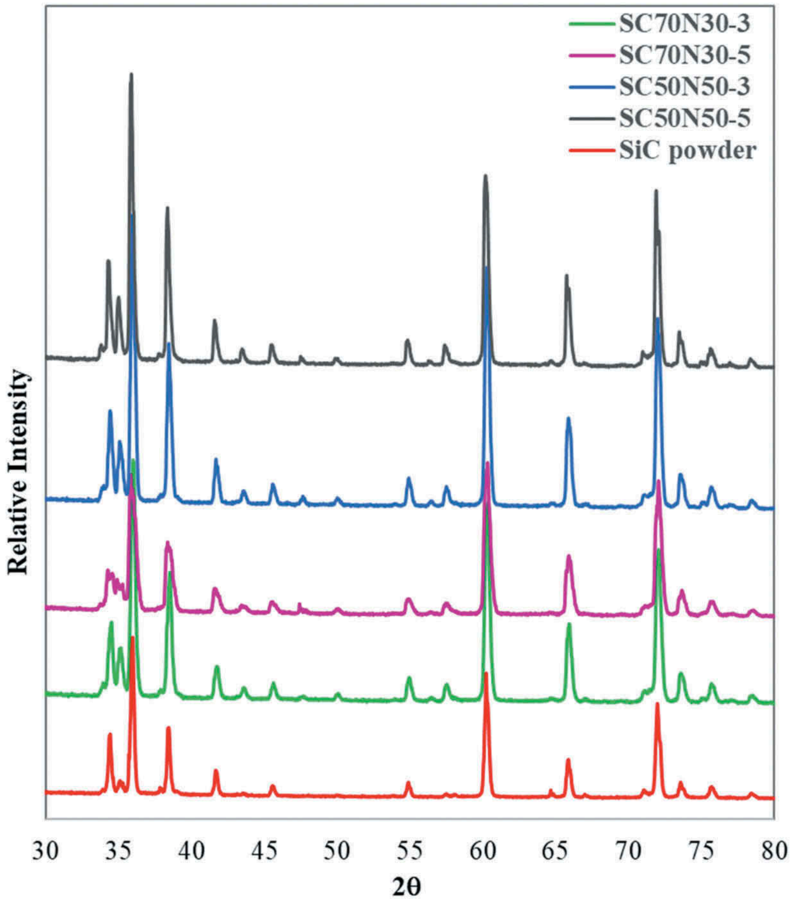

Figure 6. XRD pattern samples sintered at 600°C and SiC powder.

formation of a significant amount of the liquid phase in the system during the sintering process. This liquid phase formation promoted densification of the porous SiC ceramics at very low sintering temperatures. In this study, two SiC borax decahydrate ratios (3:1 and 5:1) were used. It was determined that, due to a large amount of borax decahydrate content in both compositons, similar sintering results were achieved.

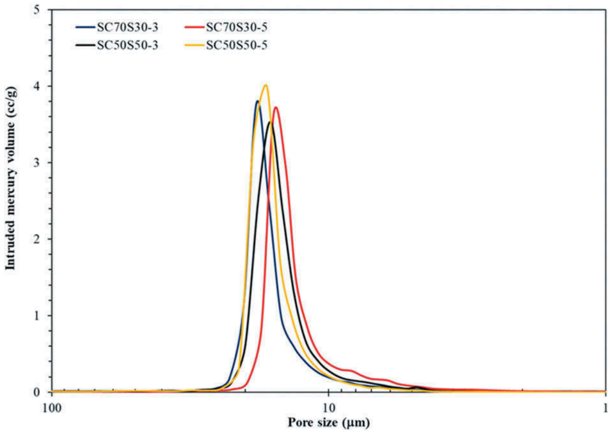

Figure 7. Pore size distribution of samples.

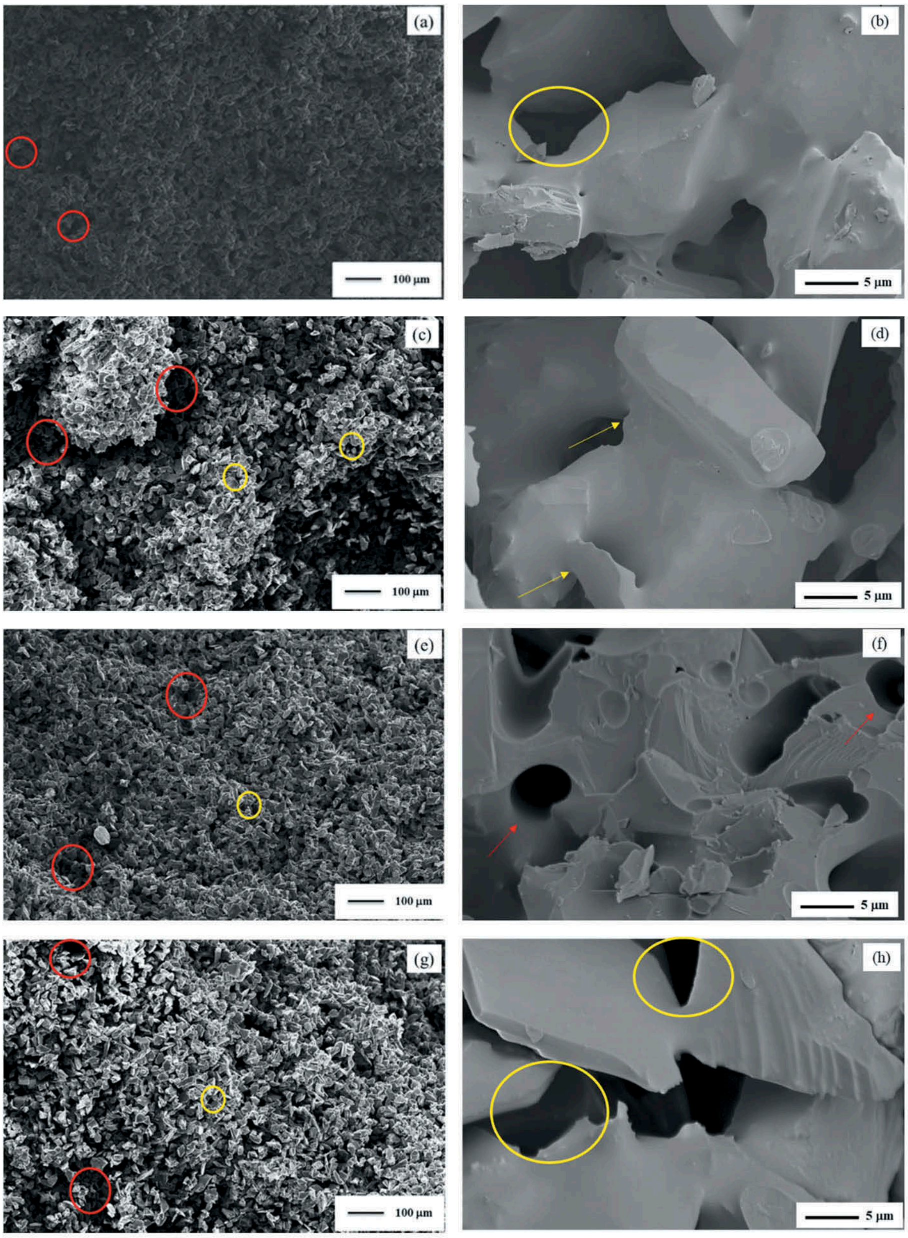

Figure 8. SEM images from fracture surfaces of samples (a, b) SC70S30–3, (c, d) SC70S30–5, (e, f) SC50S50–3 and (g, h) SC50S50–5.

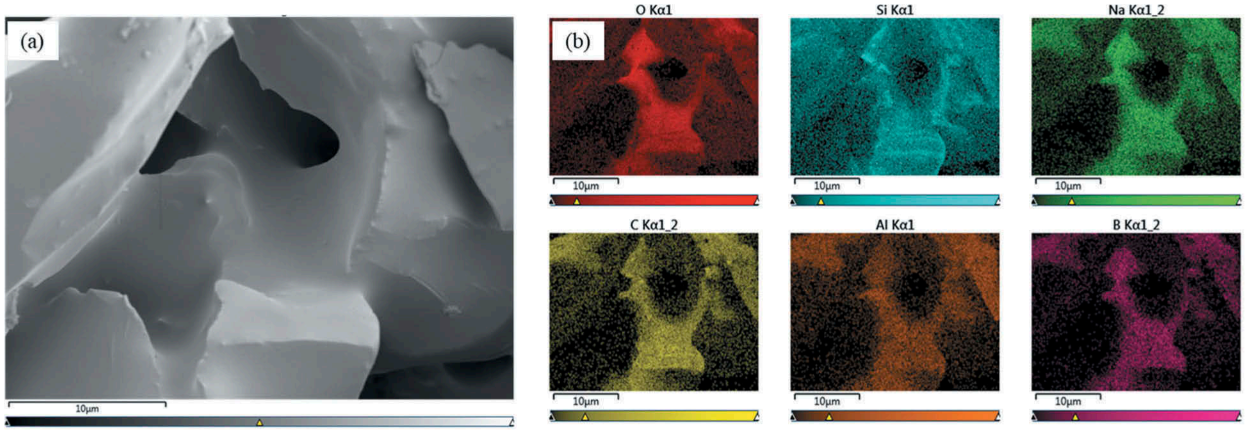

Figure 9. Representative SEM image and elemental map analysis of sample SC70S30–3.

Table 2. Elemental composition of all samples from SEM-EDX mapping study.

	Element (wt.%)					
Denomination	Si	C	O	Na	Al	B
SC70S30–3	16.0	10.4	61.5	4.3	2.5	5.4
SC70S30–5	23.2	7.0	59.3	3.2	2.3	5.0
SC50S50–3	14.9	10.6	61.9	4.6	2.0	6.0
SC50S50–5	19.8	8.6	60.5	3.1	2.9	5.2

Acknowledgments

The authors wish to thank The Scientific and Technological Research Council of Turkey (TÜBİTAK Project No: 114M510) for its financial support of this study.

Disclosure statement

No potential conflict of interest was reported by the authors.

Funding

This work was supported by the Scientific and Technological Research Council of Turkey (TÜBİTAK Project No: 114M510).

References

[1] Li QS, Zhang YJ, Gong HY, et al. Enhanced fracture toughness of pressureless-sintered SiC ceramics by addition of graphene. J Mater Sci Technol. 2016;32(7):633–638.

[2] Pastila PH, Helanti V, Nikkila AP, et al.. Chapter 5, Effect of crystallization on creep of clay bonded SiC-filters. 22nd Annual Conference on Composites, Advanced Ceramics, Materials, and Structures: B: Ceramic Engineering and Science Proceedings; Cocoa Beach, Florida. The American Ceramic Society; 1998. p. 37–44.

[3] Eom J–H, Kim Y–W, Song I–H. Effects of the initial α–siC content on the microstructure, mechanical properties, and permeability of macroporous silicon carbide ceramics. J Eur Ceram Soc. 2012;32(6):1283–1290.

[4] Chae S–H, Kim Y–W, Song I–H, et al. Porosity control of porous silicon carbide ceramics. J Eur Ceram Soc. 2009;29(13):2867–2872.

[5] Singh M, Salem J. Mechanical properties and microstructure of biomorphic silicon carbide ceramics fabricated from wood precursors. J Eur Ceram Soc. 2002;22(14):2709–2717.

[6] Eom J–H, Kim Y–W, Raju S. Processing and properties of macroporous silicon carbide ceramics: a review. J Asian Ceram Soc. 2013;1(3):220–242.

[7] Kizling MB, Stenius P, Andersson S, et al. Characterization and catalytic activity of silicon–carbide powder as catalyst support in exhaust catalysts. Appl Catal B–Environ. 1992;1(3):149–168.

[8] Pesant L, Matta J, Garin F, et al. A high–performance Pt/P–siC catalyst for catalytic combustion of model carbon particles (CPs). Appl Catal A–Gen. 2004;266(1):21–27.

[9] Keller N, Pham–Huu C, Ledoux MJ. Continuous process for selective oxidation of H2S over SiC–supported iron catalysts into elemental sulfur above its dewpoint. Appl Catal A–Gen. 2001;217(1–2):205–217.

[10] Adler J. Ceramic diesel particulate filters. Int J Appl Ceram Tech. 2005;2(6):429–439.

[11] Ichikawa S, Uchida Y, Otsuka A, et al. Material development of high porous SiC for catalyzed diesel particulate filters. SAE International in United States; 2003. (Technical Paper; No. 0148–7191: SAE).

[12] Mujeebu MA, Abdullah M, Bakar MA, et al. Applications of porous media combustion technology – a review. Appl Energy. 2009;86(9):1365–1375.

[13] Scheffler M, Colombo P. Cellular ceramics: structure, manufacturing, properties and applications. KGaA, Weinheim: WILEY-VCH Verlag GmbH & Co.; 2006.

[14] Passalacqua E, Freni S, Barone F. Alkali resistance of tape–cast SiC porous ceramic membranes. Mater Lett. 1998;34(3):257–262.

[15] Suwanmethanond V, Goo E, Liu PK, et al. Porous silicon carbide sintered substrates for high-temperature membranes. Ind Eng Chem Res. 2000;39(9):3264–3271.

[16] She J, Deng Z, Daniel–Doni J, et al. Oxidation bonding of porous silicon carbide ceramics. J Mater Sci. 2002;37(17):3615–3622.

[17] She J, Ohji T, Kanzaki S. Oxidation bonding of porous silicon carbide ceramics with synergistic performance. J Eur Ceram Soc. 2004;24(2):331–334.

[18] She J, Yang JF, Kondo N, et al. High-strength porous silicon carbide ceramics by an oxidation-bonding technique. J Am Ceram Soc. 2002;85(11):2852–2854.

[19] Zhu X, Jiang D, Tan S. Preparation of silicon carbide reticulated porous ceramics. Mater Sci Eng A. 2002;323(1):232–238.

[20] Ding S, Zhu S, Zeng Y–P, et al. Fabrication of mullite-bonded porous silicon carbide ceramics by in situ reaction bonding. J Eur Ceram Soc. 2007;27(4):2095–2102.

[21] Liu S, Zeng Y–P, Jiang D. Fabrication and characterization of cordierite-bonded porous SiC ceramics. Ceram Int. 2009;35(2):597–602.

[22] Ding S, Zeng Y–P, Jiang D. In-situ reaction bonding of porous SiC ceramics. Mater Charact. 2008;59 (2):140–143.

[23] Ding S, Zhu S, Zeng Y, et al. Effect of Y_2O_3 addition on the properties of reaction-bonded porous SiC ceramics. Ceram Int. 2006;32(4):461–466.

[24] Shi W, Liu B, Deng X, et al. In-situ synthesis and properties of cordierite-bonded porous SiC membrane supports using diatomite as silicon source. J Eur Ceram Soc. 2016;36:3465–3472.

[25] Liu S, Zeng Y, Jiang D. Effects of CeO_2 addition on the properties of cordierite-bonded porous SiC ceramics. J Eur Ceram Soc. 2009;29(9):1795–1802.

[26] Ding S, Zeng Y–P, Jiang D. Thermal shock resistance of in situ reaction bonded porous silicon carbide ceramics. Mater Sci Eng A. 2006;425(1–2):326–329.

[27] Kalemtas A. Low-temperature sintering of porous ceramics via sodium borate addition. Mat Sci Res India. 2019;16(1):48–55.

[28] Lin Y–J, Tsang C–P. Fabrication of mullite/SiC and mullite/zirconia/SiC composites by 'dual' in-situ reaction syntheses. Mater Sci Eng A. 2003;344 (1–2):168–174.

[29] Lim K–Y, Kim Y–W, Song I–H. Porous sodium borate-bonded SiC ceramics. Ceram Int. 2013;39 (6):6827–6834.

[30] Yao XM, Huang ZR, Tan SH. Preparation of silicon carbide reticulated porous ceramics sintered at low temperature with PCS as sintering additive. J Inorg Mater. 2010;25(2):168–172.

[31] Ohji T, Fukushima M. Macro-porous ceramics: processing and properties. Int Mater Rev. 2012;57(2):115–131.

[32] Yang J–F, Zhang G–J, Ohji T. Porosity and microstructure control of porous ceramics by partial hot pressing. J Mater Res. 2001;16(7):1916–1918.

[33] Caruso F, Shi X, Caruso RA, et al. Hollow titania spheres from layered precursor deposition on sacrificial colloidal core particles. Adv Mater. 2001;13(10):740–744.

[34] Wang F, Yin JW, Yao DX, et al. Fabrication of porous SiC ceramics through a modified gelcasting and solid state sintering. Mater Sci Eng A. 2016;654:292–297.

[35] Mouazer R, Thijs I, Mullens S, et al. SiC foams produced by gel casting: synthesis and characterization. Adv Eng Mater. 2004;6(5):340–343.

[36] Wang SF, Wang CA, Sun JL, et al. Fabrication, structure and properties of porous SiC ceramics with high porosity and high strength. Chin Ceram Commun. 2010;105–106:608.

[37] Eom JH, Kim YW, Song IH, et al. Processing and properties of polysiloxane-derived porous silicon carbide ceramics using hollow microspheres as templates. J Eur Ceram Soc. 2008;28(5):1029–1035.

[38] Qian J–M, Wang J–P, Qiao G–J, et al. Preparation of porous SiC ceramic with a woodlike microstructure by sol–gel and carbothermal reduction processing. J Eur Ceram Soc. 2004;24(10):3251–3259.

[39] Qian JM, Wang JP, Qiao GJ, et al. Preparation of porous SiC ceramic with a woodlike microstructure by sol–gel and carbothermal reduction processing. J Eur Ceram Soc. 2004;24(10–11):3251–3259.

[40] Singh M, Salem JA. Mechanical properties and microstructure of biomorphic silicon carbide ceramics fabricated from wood precursors. J Eur Ceram Soc. 2002;22 (14–15):2709–2717.

[41] Vogt U, Herzog A, Graule T, et al. Porous ceramics derived from wood. Key Eng Mater. 2002;206–213:1941–1944.

[42] Wang F, Yao DX, Xia YF, et al. Porous SiC ceramics prepared via freeze-casting and solid state sintering. Ceram Int. 2016;42(3):4526–4531.

[43] Xue FD, Zhou KC, Wu N, et al. Porous SiC ceramics with dendritic pore structures by freeze casting from chemical cross–linked polycarbosilane. Ceram Int. 2018;44 (6):6293–6299.

[44] Tang J, Chen YF, Wang H, et al. Preparation of oriented porous silicon carbide bodies by freeze-casting process. Key Eng Mater. 2005;280–283:1287–1290.

[45] Dey A, Kayal N, Chakrabarti O. Preparation of porous SiC ceramics by an infiltration technique. Ceram Int. 2011;37(1):223–230.

[46] Baitalik S, Dalui S, Kayal N. Mechanical and microstructural properties of cordierite-bonded porous SiC ceramics processed by infiltration technique using various pore formers. J Mater Sci. 2018;53(9):6350–6365.

[47] Qian JM, Jin ZH, Wang XW. Porous SiC ceramics fabricated by reactive infiltration of gaseous silicon into charcoal. Ceram Int. 2004;30(6):947–951.

[48] Fukushima M, Colombo P. Silicon carbide-based foams from direct blowing of polycarbosilane. J Eur Ceram Soc. 2012;32(2):503–510.

[49] Ma Y, Ma QS, Chen ZH. Low-temperature fabrication and characterization of porous SiC ceramics using preceramic polymer as binder. Rare Metal Mater Eng. 2007;36:531–533.

[50] Nghiem QD, Asthana A, Sung IK, et al. Fabrication of porous SiC-based ceramic microchannels via pyrolysis of templated preceramic polymers. J Mater Res. 2006;21(6):1543–1549.

[51] Zhu SM, Ding SQ, Xi HA, et al. Low-temperature fabrication of porous SiC ceramics by preceramic polymer reaction bonding. Mater Lett. 2005;59(5):595–597.

[52] Thunemann M, Herzog A, Vogt U, et al. Porous SiC-preforms by intergranular binding with preceramic polymers. Adv Eng Mater. 2004;6(3):167–172.

[53] Lyckfeldt O, Ferreira JMF. Processing of porous ceramics by 'starch consolidation'. J Eur Ceram Soc. 1998;18(2):131–140.

[54] Zang WJ, Jia T, Dong X. et al. Preparation of homogeneous mullite-based fibrous ceramics by starch consolidation. J Am Ceram Soc. 2018;101(7):3138–3147.

[55] Sandoval ML, Talou MH, Martinez AGT, et al. Porous cordierite-based ceramics processed by starch consolidation casting – microstructure and high-temperature mechanical behavior. Ceram Int. 2018;44(4):3893–3903.

[56] Talou MH, Camerucci MA. Processing of porous mullite ceramics using novel routes by starch consolidation casting. J Eur Ceram Soc. 2015;35(3):1021–1030.

[57] Sandoval ML, Talou MH, Martinez AGT, et al. Starch consolidation casting of cordierite precursor mixtures rheological behavior and green body properties. J Am Ceram Soc. 2015;98(10):3014–3021.

[58] Ahmed YMZ, Ewais EMM, El–Sheikh SM. Potato starch consolidation of aqueous HA suspension. J Asian Ceram Soc. 2015;3(1):108–115.

[59] Menchavez RL, Adavan CRM, Calgas JM. Starch consolidation of red clay-based ceramic slurry inside

a pressure-cooking system. Mater Res–Ibero–Am J. 2014;17(1):157–167.

[60] Gong LL, Wang YH, Cheng XD, et al. Porous mullite ceramics with low thermal conductivity prepared by foaming and starch consolidation. J Porous Mat. 2014;21(1):15–21.

[61] Ahmed YMZ, Ewais EMM, El–Sheikh SM. Effect of dispersion parameters on the consolidation of starch-loaded hydroxyapatite slurry. Process Appl Ceram. 2014;8(3):127–135.

[62] Musilova A, Gregorova E, Pabst W. Characterization of alumina–mullite–starch composites made by starch consolidation casting. Int C Polysacch Glyc. 9:166–170.

[63] Mesquita RM, Bressiani AHA. Production of porous silicon carbide ceramics by starch consolidation technique. Mater Sci Forum. 2012;727–728:821–825.

[64] Almeida FA, Botelho EC, Melo FCL, et al. Influence of cassava starch content and sintering temperature on the alumina consolidation technique. J Eur Ceram Soc. 2009;29(9):1587–1594.

[65] Qi JQ, Huang Y, Ouyang SX, et al. Fabrication of porous alumina ceramics by starch consolidation. Rare Metal Mater Eng. 2007;36:337–340.

[66] Yang DJ, You CK, Kim JW, et al. Preparation of biodegradable porous calcium metaphosphate granules as bone filler by starch consolidation. Bioceramics. 2005;17:284–286, 369–372.

[67] Pabst W, Tynova E, Mikac J, et al. A model for the body formation in starch consolidation casting. J Mater Sci Lett. 2002;21(14):1101–1103.

[68] Bowden ME, Rippey MS. Porous ceramics formed using starch consolidation. Key Eng Mater. 2002;206–213:1957–1960.

[69] Alves HM, Tari G, Fonseca AT, et al. Processing of porous cordierite bodies by starch consolidation. Mater Res Bull. 1998;33(10):1439–1448.

[70] Colombo P, Bernardo E, Biasetto L. Novel microcellular ceramics from a silicone resin. J Am Ceram Soc. 2004;87(1):152–154.

[71] Eom J–H, Kim Y–W. Effect of template size on microstructure and strength of porous silicon carbide ceramics. J Ceram Soc Jpn. 2008;116 (1358):1159–1163.

[72] Palav T, Seetharaman K. Mechanism of starch gelatinization and polymer leaching during microwave heating. Carbohydr Polym. 2006;65(3):364–370.